

Homogenization analysis of calcium leaching in concrete. A separation of scales approach

V.H. Nguyen & B. Nedjar & H. Colina

LAMI - ENPC/LCPC/Institut Navier, Cité Descartes, Marne-la-vallée Cedex2, France.

J. M. Torrenti

IRSN/DIR/Pg, Fontenay-aux-Roses Cedex, France.

ABSTRACT: We present in this work a modeling of calcium leaching in concrete by taking into account the influence of the presence of aggregate. The modeling consists of the derivation of the microscopic equation governing the average concentration field in the equivalent medium as well as the determination of the macroscopic transport parameters. The homogenization method allows to estimate the diffusion and tortuosity tensor to be introduced in the macroscopic formulation of mass conservation law. These estimates depend on the morphological parameters of the microstructure which represent the geometry of the domain occupied by the phase in which the diffusion process takes places. The problem of numerically integrating the equations at hand is addressed within the context of the finite element method. Finally, numerical simulations are compared with experimental results on concrete.

Keywords: calcium leaching, homogenization, periodicity, asymptotic development, concrete.

1 INTRODUCTION

Concrete is commonly employed in radioactive waste disposal, and then, besides carrying the mechanical loadings, concrete containment structures must also ensure the load-bearing capacity over extended periods depending on the level of radioactivity.

Phenomenological approaches can be used to describe the chemical behavior of mortar and cement paste. In this work, we consider the nowadays well known simplified approach of calcium leaching, see (Carde et al. 1996; Gerard 1996; Torrenti et al. 1998; Ulm et al. 1999; Bangert et al; 2001) among many other references.

However, when considering the concrete material, the effects of the aggregates must be accounted for. Although the mechanism of calcium leaching in the microscale has been well established, i.e. in the scale of the Elementary Representative Volume (ERV), it is practically impossible to solve the full equations for the complex microscale geometries.

To overcome these difficulties, the heterogeneous concrete media can be treated as an equivalent homogeneous one. In this paper, the

macroscopic equivalent equations are derived by a homogenization method based on the well known double-scale asymptotic development approach, see (Bensoussan et al. 1978; Sanchez-Palencia 1980; Auriault & Lewandowska 1996).

The general idea of the homogenization process is the shift from the description of the phenomenon at the microscale (the ERV scale), where the governing equations are given, to the equivalent macroscopic boundary problem that provides the averaged behavior of the equivalent medium.

The paper is organized as follows. In the next section the calcium leaching problem of mortar and cement paste is described, then the homogenization method is described in section 3. The numerical design within the context of the finite element method is described in section 4, and finally, in section 5, numerical simulations are compared with experimental data.

2 CALCIUM LEACHING OF CEMENT PASTE

During the last few years, different models have been developed to describe the calcium leaching process. For cement-based materials (cements pastes and mortar), the kinetic of calcium leaching

is determined from the mass conservation of calcium which describes the evolution of the amount of calcium in the liquid phase of the material. One has the following macroscopic balance of the calcium ion mass:

$$\frac{\partial}{\partial t} [(\phi(c)c) + s(c)] = \text{div}[\tilde{D}(c)\mathbf{grad}c], \quad (1)$$

where $\text{div}[\cdot]$ and $\mathbf{grad}[\cdot]$ denote the divergence and the gradient operators respectively. c is the calcium concentration in liquid phase, s is the calcium concentration in solid phase, ϕ is the porosity in material, and $\tilde{D}(c)$ denotes the apparent calcium ion conductivity. According to (Gérard 1996), this simplified approach focuses on the evolution of one variable only, namely: the calcium concentration c . That is, all the quantities s , ϕ and $\tilde{D}(c)$ may depend on the (state) variable c . As an illustration, Figures 1-3 give these dependencies for a mortar material.

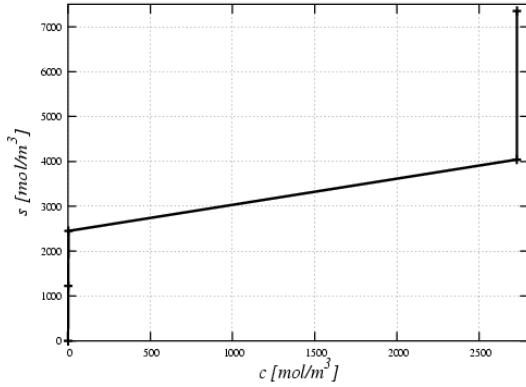


Figure 1: Chemical equilibrium $s(c)$ for accelerated ammonium nitrate calcium leaching in mortar.

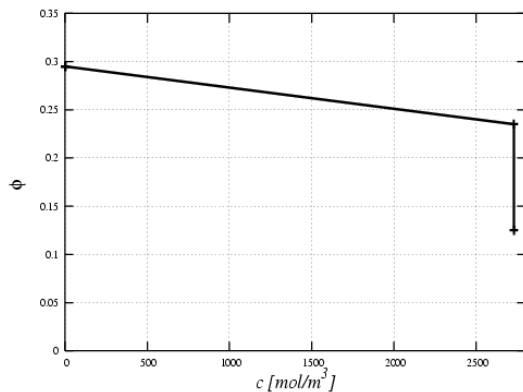


Figure 2: Porosity ϕ versus the calcium concentration c for mortar.

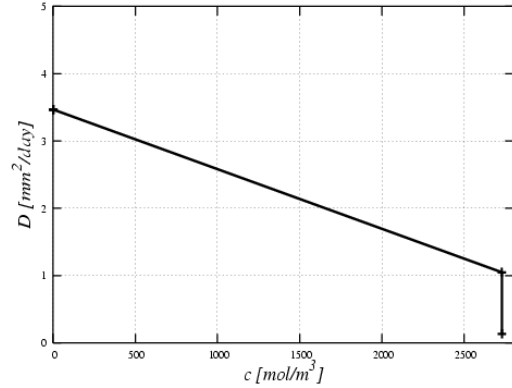


Figure 3: Apparent conductivity $\tilde{D}(c)$ versus the calcium concentration c in mortar.

The problem of numerically integrating this highly nonlinear problem is treated in numerous publications. However, when applied to concrete, some difficulties appear because the aggregates play a determining role in the calcium leaching process (the tortuosity, the heterogeneity, the volume fraction effects ...). In this work, we choose to treat the heterogeneous concrete material as an equivalent homogeneous medium at the macroscale by using a homogenization method.

3 HOMOGENIZATION METHOD

The general idea of the homogenization process is the shift from the description of the phenomenon at the micro-scale (ERV scale), where the governing equations are given, to the equivalent macroscopic boundary value problem that provides the averaged behavior of the equivalent medium.

In our case, concrete is considered as a mixture of a homogeneous matrix of mortar which leaches, and aggregates which do not leach (silicate based aggregates).

The basic assumption is the existence of an ERV of the medium, which is small in comparison with the macroscopic volume. In a periodic medium, the ERV represents the periodic cell. Let l be its characteristic length, and L be a characteristic macroscopic length. The separation of scales is represented by the small parameter ε defined as the ratio of the scale of the ERV and the scale of the structure.

$$\varepsilon = \frac{l}{L} \ll 1 \quad (2)$$

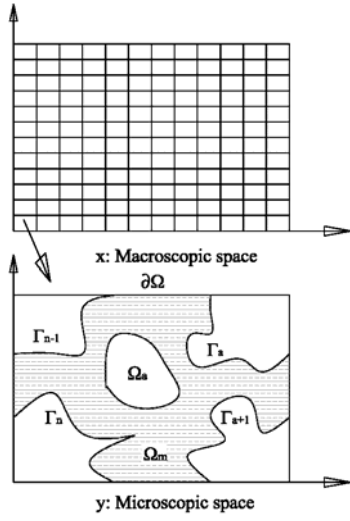


Figure 4: Concrete structure. Separation of scales.

In this analysis, the concrete is considered as a periodic medium (see Fig. 4). In the unit cell Ω , Ω_m is the matrix of mortar, Ω_a is the aggregates volume, and Γ_a is the boundary between the aggregates and the matrix. The aggregates are assumed to not leach.

Within the framework of the phenomenological approach, the mass balance equation for the calcium leaching in Ω can be described by:

$$\frac{\partial}{\partial t} \tilde{S}(c) = \text{div} \left[\tilde{D}(c) \mathbf{grad} c \right] \quad \text{in } \Omega_m \quad (3)$$

$$\mathbf{N} \cdot \tilde{D}(c) \mathbf{grad} c = 0 \quad \text{on } \Gamma_a \quad (4)$$

where the $\text{div}[\cdot]$ and $\mathbf{grad}[\cdot]$ operators are expressed relative to the microscopic scale \mathbf{y} , and where, and in all what follows, we have introduced the notation $\tilde{S}(c) = \phi(c)c + s(c)$ (see (1)). \mathbf{N} is the outward unit vector normal to Γ_a . Equation (4) reflects the fact that there is no leaching in the aggregates (impermeability condition).

Now the problem can be formulated as follows. Supposing that the governing equations of leaching are known, determine the macroscopic leaching equation and the definition of the macroscopic parameters for the equivalent continuous medium.

Normalization

In the process of homogenization all the variables will be normalized with respect to the characteristic length l . Following the same idea as in (Auriault and Lewandowska 1996), equations (3) and (4) give a dimensionless number P which provides a measure of the relative influence

between the transient and the diffusion phenomena incorporated in the analysis. It provides the condition for the case where homogenization is not possible.

$$P = \frac{\left| \frac{\partial \tilde{S}(c)}{\partial t} \right|}{\left[\frac{\partial}{\partial X_i} \left[\tilde{D}(c) \frac{\partial}{\partial X_j} c \right] \right]} \quad (5)$$

According to (Auriault and Lewandowska 1996), the case $P = O(\varepsilon^2)$ will be adopted here. That is, the problem (3)-(4) in the microscopic scale is now given by:

$$\varepsilon^2 \frac{\partial \tilde{S}(c)}{\partial t} - \frac{\partial}{\partial y_i} \left[\tilde{D}(c) \frac{\partial c}{\partial y_j} \right] = 0 \quad \text{in } \Omega_m \quad (6)$$

$$N_i \tilde{D}(c) \frac{\partial c}{\partial y_j} = 0 \quad \text{on } \Gamma_a \quad (7)$$

Due to the separation of scales, the calcium concentration field c is now function of three variables, i.e. $c = c(\mathbf{x}, \mathbf{y}, t)$, where \mathbf{y} is the microscopic (fast) space variable, $\mathbf{x} = \varepsilon \mathbf{y}$ is the macroscopic (slow) space variable and t is the time variable. Following the homogenization procedure, it is assumed that $c(\mathbf{x}, \mathbf{y}, t)$ can be presented in the form of an asymptotic development given by

$$c(\mathbf{x}, \mathbf{y}, t) = c^0(\mathbf{x}, \mathbf{y}, t) + \varepsilon c^1(\mathbf{x}, \mathbf{y}, t) + \varepsilon^2 c^2(\mathbf{x}, \mathbf{y}, t) + \varepsilon^3 c^3(\mathbf{x}, \mathbf{y}, t) + \dots \quad (8)$$

Where the component $c^{(i)}(\mathbf{x}, \mathbf{y}, t)$ are \mathbf{y} -periodic and the variable \mathbf{x} is expressed function of the variable \mathbf{y} ($\mathbf{x} = \varepsilon \mathbf{y}$). Again, this latter means that the microscopic point of view is adopted, and implies that the gradient operator becomes:

$$\frac{\partial}{\partial \mathbf{y}} c(\mathbf{x}(\mathbf{y}), \mathbf{y}) = \left(\frac{\partial}{\partial \mathbf{y}} + \varepsilon \frac{\partial}{\partial \mathbf{x}} \right) c \quad (9)$$

Similarly, the calcium concentration in the solid phase and the apparent calcium conductivity can be expressed in forms similar to (8). These can be written as:

$$\tilde{S}(c) = \tilde{S}(c^0) + \varepsilon c^1 \frac{\partial \tilde{S}(c^0)}{\partial c^0} + \varepsilon^2 c^2 \frac{\partial \tilde{S}(c^0 + \varepsilon c^1)}{\partial (c^0 + \varepsilon c^1)} + \dots \quad (10)$$

$$\begin{aligned} \tilde{D}(c) = \tilde{D}(c^0) + \varepsilon c^1 \frac{\partial \tilde{D}(c^0)}{\partial c^0} \\ + \varepsilon^2 c^2 \frac{\partial \tilde{D}(c^0 + \varepsilon c^1)}{\partial (c^0 + \varepsilon c^1)} + \dots \end{aligned} \quad (11)$$

The methodology of the homogenization resides in the application of the asymptotic developments (8), (10) and (11) into (6) and (7). Comparison of the terms of the same power of ε will yield the required descriptions in the form of the systems of equations to be analyses.

Comparison of the corresponding terms gives at the ε^0 order:

$$\frac{\partial}{\partial y_i} \left[\tilde{D}(c^0) \frac{\partial c^0}{\partial y_j} \right] = 0 \quad \text{in } \Omega_m \quad (12)$$

$$N_i \tilde{D}(c^0) \frac{\partial c^0}{\partial y_j} = 0 \quad \text{on } \Gamma_a \quad (13)$$

At the ε^1 the cell problem takes the form:

$$\begin{aligned} \frac{\partial}{\partial y_i} \left[c^1 \tilde{D}(c^0) \frac{\partial c^0}{\partial y_i} + \tilde{D}(c^0) \left(\frac{\partial c^0}{\partial x_i} + \frac{\partial c^1}{\partial y_i} \right) \right] \\ + \frac{\partial}{\partial x_i} \left[\tilde{D}(c^0) \frac{\partial c^0}{\partial y_i} \right] = 0 \quad \text{in } \Omega_m \end{aligned} \quad (14)$$

$$\begin{aligned} N_i \left[\tilde{D}(c^0) \left(\frac{\partial c^0}{\partial x_i} + \frac{\partial c^1}{\partial y_i} \right) + c^1 \frac{\partial \tilde{D}(c^0)}{\partial c^0} \frac{\partial c^0}{\partial y_i} \right] \\ = 0 \quad \text{on } \Gamma_a \end{aligned} \quad (15)$$

And, at the next order ε^2 the problem is:

$$\begin{aligned} \frac{\partial \tilde{S}(c^0)}{\partial t} - \frac{\partial}{\partial x_i} \left[c^1 \tilde{D}(c^0) \frac{\partial c^0}{\partial y_i} \right] \\ - \frac{\partial}{\partial x_i} \left[\tilde{D}(c^0) \left(\frac{\partial c^0}{\partial x_j} + \frac{\partial c^1}{\partial y_j} \right) \right] \\ - \frac{\partial}{\partial y_i} \left[\tilde{D}(c^0) \left(\frac{\partial c^1}{\partial x_i} + \frac{\partial c^2}{\partial y_i} \right) \right] \\ - \frac{\partial}{\partial y_i} \left[c^1 \frac{\partial \tilde{D}(c^0)}{\partial c^0} \left(\frac{\partial c^0}{\partial x_i} + \frac{\partial c^1}{\partial y_i} \right) \right] \\ - \frac{\partial}{\partial y_i} \left[c^2 \frac{\partial \tilde{D}(c^0 + \varepsilon c^1)}{\partial (c^0 + \varepsilon c^1)} \frac{\partial c^0}{\partial y_i} \right] = 0 \quad \text{in } \Omega_m \end{aligned} \quad (16)$$

$$\begin{aligned} N_i \left[\tilde{D}(c^0) \left(\frac{\partial c^1}{\partial x_i} + \frac{\partial c^2}{\partial y_i} \right) \right] \\ + N_i \left[c^1 \frac{\partial \tilde{D}(c^0)}{\partial c^0} \left(\frac{\partial c^0}{\partial x_i} + \frac{\partial c^1}{\partial y_i} \right) \right] \\ + N_i \left[c^2 \frac{\partial \tilde{D}(c^0 + \varepsilon c^1)}{\partial (c^0 + \varepsilon c^1)} \frac{\partial c^0}{\partial y_i} \right] = 0 \quad \text{on } \Gamma_a \end{aligned} \quad (17)$$

Multiplying equation (12) by c^0 , integrating over the matrix Ω_m , and then using the divergence theorem together with the periodic boundary conditions (13) leads to the following expression

$$\int_{\Omega_m} \tilde{D}(c^0) \frac{\partial c^0}{\partial y_i} \frac{\partial c^0}{\partial y_i} d\Omega = 0. \quad (18)$$

Then, from the positivity of the positive of the apparent coefficient of diffusivity $\tilde{D}(c^0) \geq 0$, it is concluded that the function c^0 depends only on the macroscopic scale \mathbf{x} , i.e.

$$c^0(\mathbf{x}, \mathbf{y}) = c^0(\mathbf{x}). \quad (19)$$

Taking into account the result (19), the system (14)-(15) reduces then to:

$$\frac{\partial}{\partial y_i} \left[\tilde{D}(c^0) \left(\frac{\partial c^0}{\partial x_i} + \frac{\partial c^1}{\partial y_i} \right) \right] \quad \text{in } \Omega_m \quad (20)$$

$$N_i \left[\tilde{D}(c^0) \left(\frac{\partial c^0}{\partial x_i} + \frac{\partial c^1}{\partial y_i} \right) \right] = 0 \quad \text{on } \Gamma_a \quad (21)$$

By linearity, one can show that the calcium concentration field satisfying the system (20)-(21) is of the form:

$$c^1(\mathbf{x}, \mathbf{y}, t) = \chi_k(\mathbf{y}) \frac{\partial c^0}{\partial x_k} + f(\mathbf{x}, t) \quad (22)$$

where $\chi_k(\mathbf{y})$ is \mathbf{y} -periodic and $\langle \chi \rangle = 0$. The latter condition means that the mean values of χ over periodic volume is equal to zero.

$$\langle \chi(\mathbf{y}) \rangle = \frac{1}{|\Omega|} \int_{\Omega} \chi(\mathbf{y}) d\Omega = 0. \quad (23)$$

In (22), $f(\mathbf{x}, t)$ is an arbitrary function of the \mathbf{x} -space. Substituting (22) into equations (20)-(21), we obtain the following local boundary value problem:

$$\frac{\partial}{\partial y_i} \left[\tilde{D}(c^0) \left(\delta_{ik} + \frac{\partial \chi_k}{\partial y_i} \right) \right] = 0 \quad \text{in } \Omega_m \quad (24)$$

$$N_i \left[\tilde{D}(c^0) \left(\delta_{ik} + \frac{\partial \chi_k}{\partial y_i} \right) \right] = 0 \quad \text{on } \Gamma_a \quad (25)$$

This problem gives the vectorial field $\boldsymbol{\chi}$ which will appear in the definition of the macroscopic equivalent diffusion tensor.

Next, using again the result (19) into the system (16)-(17) leads to the following one:

$$\begin{aligned} \frac{\partial \tilde{S}(c^0)}{\partial t} - \frac{\partial}{\partial x_i} \left[\tilde{D}(c^0) \left(\frac{\partial c^0}{\partial x_i} + \frac{\partial c^1}{\partial y_i} \right) \right] \\ - \frac{\partial}{\partial y_i} \left[\tilde{D}(c^0) \left(\frac{\partial c^1}{\partial x_i} + \frac{\partial c^2}{\partial y_i} \right) \right] \\ - \frac{\partial}{\partial y_i} \left[c^1 \frac{\partial \tilde{D}(c^0)}{\partial c^0} \left(\frac{\partial c^0}{\partial x_i} + \frac{\partial c^1}{\partial y_i} \right) \right] \\ = 0 \quad \text{in } \Omega_m \end{aligned} \quad (26)$$

$$\begin{aligned} N_i \left[\tilde{D}(c^0) \left(\frac{\partial c^1}{\partial x_i} + \frac{\partial c^2}{\partial y_i} \right) \right] \\ + N_i \left[c^1 \frac{\partial \tilde{D}(c^0)}{\partial c^0} \left(\frac{\partial c^0}{\partial x_i} + \frac{\partial c^1}{\partial y_i} \right) \right] = 0 \quad \text{on } \Gamma_a \end{aligned} \quad (27)$$

Moreover, the system (26)-(27) can be simplified as follows. Integrating (26) over Ω_m , use on the divergence theorem together with the boundary condition (27) and the periodicity over Ω , and finally by dividing the result by the measure of Ω , leads to:

$$\begin{aligned} \frac{1}{\Omega} \int_{\Omega_m} \frac{\partial \tilde{S}(c^0)}{\partial t} d\Omega \\ - \frac{1}{\Omega} \int_{\Omega_m} \frac{\partial}{\partial x_i} \left[\tilde{D}(c^0) \left(\frac{\partial c^0}{\partial x_i} + \frac{\partial c^1}{\partial y_i} \right) \right] d\Omega = 0 \end{aligned} \quad (28)$$

Now taking again into account the expression (22) into (28), the calcium leaching in the equivalent macroscopic media is given by:

$$f_m \frac{\partial \tilde{S}(c^0)}{\partial t} - \frac{\partial}{\partial x_i} \left(\langle \mathbf{D}(c^0) \rangle \frac{\partial c^0}{\partial x_k} \right) = 0 \quad (29)$$

where,

$$f_m = \frac{1}{\Omega} \int_{\Omega_m} d\Omega \quad (30)$$

is the volume fraction of the mortar. And the average macroscopic apparent diffusion tensor is given by:

$$\langle \mathbf{D}(c^0) \rangle = \tilde{D}(c^0) \tau_{ik} = \frac{1}{\Omega} \int_{\Omega} \tilde{D}(c^0) \left[\left(\delta_{ik} + \frac{\partial \chi_k}{\partial y_i} \right) \right] d\Omega \quad (31)$$

where

$$\tau_{ik} = \frac{1}{\Omega} \int_{\Omega} \left[\left(\delta_{ik} + \frac{\partial \chi_k}{\partial y_i} \right) \right] d\Omega \quad (32)$$

are the components of the tortuosity tensor.

Summary:

In summary, the solution of a problem of calcium leaching in concrete should be carried out in three steps: (i) First, the local boundary value problem (24)-(25) for a periodic cell should be solved, giving the vector field $\boldsymbol{\chi}$ with components χ_i ($i = 1, 2$ for a two-dimension problem). (ii) Second, the equivalent apparent diffusion tensor should then be calculated according to its definition (31)-(32). And in (iii), the final step consists of resolving the boundary value problem (29) for the equivalent medium in the macro-scale, subject to the given initial and boundary conditions.

Steps (i) and (ii) are easy to perform within a finite element method framework. Problem (24)-(25) is linear and is solved once and for all for a given periodic cell (the ERV). In step (iii), the boundary value problem (29) is highly nonlinear (as its counterpart in (1)). In the next section we give a description of the algorithm we use to numerically solve it in this work.

4 NUMERICAL ALGORITHM OF CALCIUM LEACHING

After determining the average diffusion (steps (i) and (ii) above), the equivalent dissolution-diffusion equation (29) is written in weak form as:

$$\int_{\Omega} \delta c f_m \frac{\partial \tilde{S}(c)}{\partial t} d\Omega + \int_{\Omega} \mathbf{grad} \delta c \cdot \tilde{D}(c) \mathbf{r} \cdot \mathbf{grad} c d\Omega = 0 \quad (33)$$

which must hold for all admissible variations δc . For simplicity, Dirichlet boundary conditions are assumed on the entire boundary $\partial\Omega$ of the medium.

Many strategies have been developed to solve this problem. The numerical resolution is based on an iterative procedure of the discrete version of

(33). Typically, this requires a linearization and, accordingly, one solves a sequence of successive linear problems. However, one can expect severe numerical difficulties and use of refined mesh is necessary because of the strong nonlinearities exhibited by $\tilde{S}(c)$ and $\tilde{D}(c)$ functions, see (Figs. 1-3). Other ways to treat this equation are, for example, to consider it as a Stefan-like problem as in (Ulm et al. 2002), or resolve it via the finite volumes method as in (Mainguy et al. 2000). In this work instead, and motivated by a recent algorithm proposed in (Nedjar 2002) within the context of nonlinear heat problems involving phase change, we employ a *relaxed* linearization as this was done in (Nedjar et al. 2003) to resolve problem (1).

4.1 Relaxed linearization.

The procedure concerns the highly nonlinear functions $\tilde{S}(c)$ and $\tilde{D}(c)$. The key idea proceeds in three steps:

In the first step, use is made of the reciprocal forms of the precedent two functions. That is, we introduce the functions:

$$c = f(\tilde{S}) \quad \text{and} \quad c = g(\tilde{D}), \quad (34)$$

which can be easily deduced from $\tilde{S}(c)$ and $\tilde{D}(c)$, respectively.

In the second step, linearizations of the above functions f and g are given by:

$$\begin{aligned} c^{(i+1)} &= f(\tilde{S}^{(i)}) + f'(\tilde{S}^{(i)})\Delta\tilde{S}^{(i)}, \\ c^{(i+1)} &= g(\tilde{D}^{(i)}) + g'(\tilde{D}^{(i)})\Delta\tilde{D}^{(i)}, \end{aligned} \quad (35)$$

Where f' and g' are the derivatives of f and g with respect to their argument. The superscripts (i) and $(i+1)$ refer to the iteration number.

The identities (35) are equivalently written as:

$$\begin{aligned} \Delta\tilde{S}^{(i)} &= \frac{1}{f'(\tilde{S}^{(i)})} [(\Delta c^{(i)} + (c^{(i)} - f(\tilde{S}^{(i)})))] \\ \Delta\tilde{D}^{(i)} &= \frac{1}{g'(\tilde{D}^{(i)})} [(\Delta c^{(i)} + (c^{(i)} - g(\tilde{D}^{(i)})))] \end{aligned} \quad (36)$$

And in the third step, the latter incrementations (36) are relaxed by replacing the quantities $1/f'(\tilde{S}^{(i)})$ and $1/g'(\tilde{D}^{(i)})$ by constant quantities μ and γ in all the domain and during the whole iterative process as:

$$\begin{aligned} \Delta\tilde{S}^{(i)} &= \mu [(\Delta c^{(i)} + (c^{(i)} - f(\tilde{S}^{(i)})))] \\ \Delta\tilde{D}^{(i)} &= \gamma [(\Delta c^{(i)} + (c^{(i)} - g(\tilde{D}^{(i)})))] \end{aligned} \quad (37)$$

The relaxation parameters and must satisfy the respective conditions:

$$\mu \leq \frac{1}{\max f'(\tilde{S}^{(i)})}, \quad \gamma \leq \frac{1}{\max g'(\tilde{D}^{(i)})} \quad (38)$$

In our numerical examples, we use:

$$\mu = 1/\max f'(\tilde{S}^{(i)}); \quad \lambda = 1/\max g'(\tilde{D}^{(i)}) \quad (39)$$

4.2 Resolution algorithm.

To solve the problem (33) using the precedent algorithmic procedure, we first perform a finite difference scheme in time. In this paper, use is made of a backward-Euler scheme as follows. Consider a typical time subinterval $[t_n, t_{n+1}]$, then, starting from a known converged state $(c_n, \tilde{S}_n, \tilde{D}_n)$ at time t_n , we look for the new state $(c_{n+1}, \tilde{S}_{n+1}, \tilde{D}_{n+1})$ at time t_{n+1} by solving:

$$\begin{aligned} \int_{\Omega} \delta c f_m \frac{\tilde{S}_{n+1}}{\Delta t} d\Omega + \int_{\Omega} \mathbf{grad} \delta c \cdot \tilde{D}_{n+1} \boldsymbol{\tau} \cdot \mathbf{grad} c_{n+1} d\Omega \\ = \int_{\Omega} \delta c f_m \frac{\tilde{S}_n}{\Delta t} d\Omega \end{aligned} \quad (40)$$

where $\Delta t = t_{n+1} - t_n$. A classical linearization of (40) gives:

$$\begin{aligned} \int_{\Omega} \delta c f_m \frac{\tilde{S}_{n+1}^{(i)}}{\Delta t} d\Omega + \int_{\Omega} \mathbf{grad} \delta c \cdot \boldsymbol{\tau} \cdot \mathbf{grad} c_{n+1}^{(i)} \Delta \tilde{D}_{n+1}^{(i)} d\Omega \\ + \int_{\Omega} \mathbf{grad} \delta c \cdot \tilde{D}_{n+1}^{(i)} \boldsymbol{\tau} \cdot \mathbf{grad} \Delta c_{n+1}^{(i)} d\Omega = R_{n+1}^{(i)} \end{aligned} \quad (41)$$

where the residual at iteration is given by:

$$\begin{aligned} R_{n+1}^{(i)} &= \int_{\Omega} \delta c f_m \frac{\tilde{S}_n^{(i)} - \tilde{S}_{n+1}^{(i)}}{\Delta t} d\Omega \\ &+ \int_{\Omega} \mathbf{grad} \delta c \cdot \tilde{D}_{n+1}^{(i)} \boldsymbol{\tau} \cdot \mathbf{grad} c_{n+1}^{(i)} d\Omega \end{aligned} \quad (42)$$

In (41) and (42), subscripts refer to the time step and superscripts refer to the iteration within the time step.

The *relaxed* linearization of the problem (33) is then obtained by replacing the increments (37) into the first and second terms of the left hand side of (41):

$$\begin{aligned}
& \int_{\Omega} \delta c \mu f_m \frac{\Delta c_{n+1}^{(i)}}{\Delta t} d\Omega + \int_{\Omega} \mathbf{grad} \delta c \cdot \gamma \boldsymbol{\tau} \cdot \mathbf{grad} c_{n+1}^{(i)} \Delta c_{n+1}^{(i)} d\Omega \\
& + \int_{\Omega} \mathbf{grad} \delta c \cdot \tilde{D}_{n+1}^{(i)} \boldsymbol{\tau} \cdot \mathbf{grad} \Delta c_{n+1}^{(i)} d\Omega \\
& = R_{n+1}^{(i)} - \int_{\Omega} \delta c \frac{\mu f_m}{\Delta t} (c_{n+1}^{(i)} - f(\tilde{S}_{n+1}^{(i)})) d\Omega \\
& + \int_{\Omega} \mathbf{grad} \delta c \cdot \boldsymbol{\tau} \cdot \mathbf{grad} c_{n+1}^{(i)} \gamma (c_{n+1}^{(i)} - g(\tilde{D}_{n+1}^{(i)})) d\Omega
\end{aligned} \tag{43}$$

At the end of each iteration, the updating procedure is accomplished as follows:

$$\begin{aligned}
c_{n+1}^{(i+1)} &= c_{n+1}^{(i)} + \Delta c_{n+1}^{(i)}, \\
\tilde{S}_{n+1}^{(i+1)} &= \tilde{S}_{n+1}^{(i)} + \mu (c_{n+1}^{(i+1)} - f(\tilde{S}_{n+1}^{(i)})), \\
\tilde{D}_{n+1}^{(i+1)} &= \tilde{D}_{n+1}^{(i)} + \mu (c_{n+1}^{(i+1)} - g(\tilde{D}_{n+1}^{(i)})).
\end{aligned} \tag{44}$$

From the finite element point of view, the update (44)₁ is accomplished at the nodal level while the updates (44)₂ and (44)₃ are performed at the integration points.

5 NUMERICAL VALIDATION

Within the context of the finite element method, the algorithm developed in section 4 has been implemented in an enhanced version of the CESAR-LCPC finite element software, see (Humbert 1989). The first section concerns the local problem of homogenization of concrete to find the tortuosity tensor, and the second section concerns the simulation of a calcium leaching test under ammonium nitrate solution. In this latter, the simulations are compared with partial experimental results obtained on concrete.

5.1 Local problem

We consider a unit cell of dimension 50x50 mm with the volume fraction of mortar $f_m=0.6$. Two morphologies of aggregates are considered: circles and triangles. The figures 4 and 5 give the adopted aggregate distributions together with, for instance, the corresponding χ_1 component of the vector field $\boldsymbol{\chi}$.

For the morphology of figure 4, the finite element computations give the following tortuosity tensor:

$$\boldsymbol{\tau}_{circle} = \begin{bmatrix} 0.42336 & 0.5616 \cdot 10^{-2} \\ 0.5616 \cdot 10^{-2} & 0.4334 \end{bmatrix} \tag{45}$$

And for the morphology of figure 5, the computations give the following one:

$$\boldsymbol{\tau}_{triangle} = \begin{bmatrix} 0.3208 & 0.2575 \cdot 10^{-4} \\ 0.2575 \cdot 10^{-4} & 0.3147 \end{bmatrix} \tag{46}$$

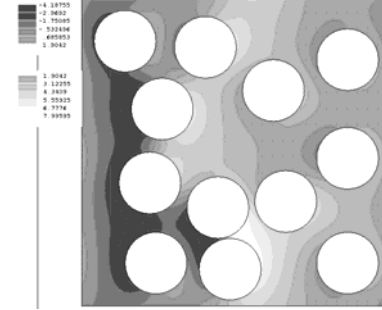


Figure 4: First morphology and the corresponding χ_1 field.

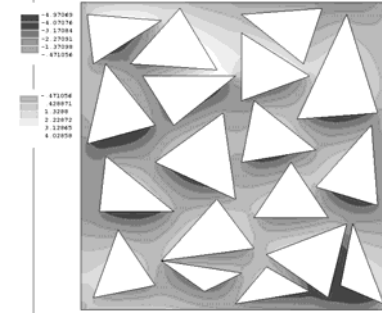


Figure 5: Second morphology and the corresponding χ_1 field.

Observe that, on one hand, these tensors are almost symmetric. This is because there is not a preferred direction of apparent calcium diffusivity. Moreover, because the non-diagonal terms are small compared to the diagonal ones (see (45) and (46)), one can consider a *scalar tortuosity* factor only for our problem. And on the other hand, one can observe that the geometries of the aggregates play an important role. In fact, while the tortuosity is about 0.42 for circular aggregates, it is about 0.32 for triangular aggregates. That is, the apparent conductivity for triangular aggregates is about 25% lesser than for circular aggregates.

5.2 Calcium leaching under ammonium nitrate solution

We consider a cylindrical specimen of concrete of external radius $R = 110$ mm and internal radius $r = 27$ mm. It is submitted to calcium leaching under ammonium nitrate solution. For the numerical simulation, we use the morphology of figure 4.

The boundary conditions consist of zero mass fluxes on the top and bottom boundaries, and of

imposed calcium concentration $c = 0$ [mol/m³] on the rest of the boundary.

The material data we use for the mortar matrix are smoothed versions of the $s(c)$, $\phi(c)$ and $\tilde{D}(c)$ curves shown in Figs. 1-3. The concrete apparent diffusivity used in (29) is $\tilde{D}_c(c) = \tilde{D}(c)\tau$. The initial condition for the calcium concentration in the liquid phase is given by $c_0(\mathbf{x}, t=0) = 2730$ mol/m³ for all $\mathbf{x} \in \Omega$ which corresponds to the initial value $s_0(\mathbf{x}, t=0) = 7350$ mol/m³ for the calcium concentration in the solid phase.

Figures 6 and 7 show the simulated degradation depths in concrete compared to the corresponding experimental results after 36 and 57 days, respectively.

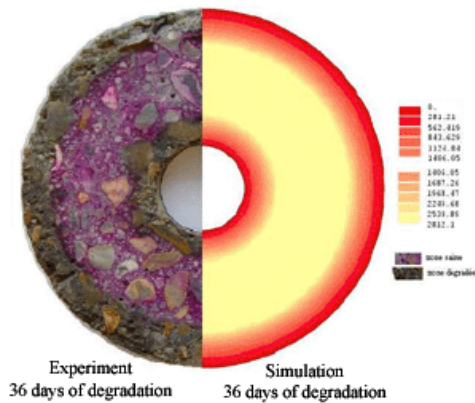


Figure 6: Degradation depth after 36 days, experimental-simulation comparison

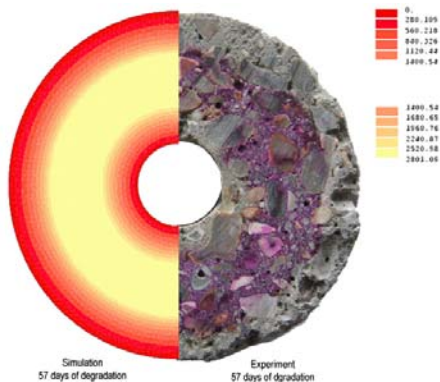


Figure 7: Degradation depth after 57 days, experimental-simulation comparison

6 CONCLUSION

We have presented in this work a two-scale approach to describe the chemical degradation in concrete materials. Use has been made of the well-

known simplified approach of calcium leaching widely employed to model cement-based materials.

The method described here is based on the two-scale asymptotic developments. We have shown how the macroscopic characteristics of the equivalent homogeneous media can be identified.

The simulations have shown that the morphological geometry of the aggregates is very important to describe the diffusivity of the calcium in the concrete.

REFERENCES

- Auriault J.L. and J. Lewandowska, (1996), *Diffusion, adsorption, advection in porous media: homogenization analysis*. Eur. J. Mechanics, A/Solids, vol. 15(4) 681-704
- Bangert F., D. Kuhl, and G. Meschke (2001). Finite element simulation of chemo-mechanical damage under cyclic loading conditions. In *Fracture Mechanics of Concrete and Structures* (R. de Borst et al., eds.), Swets and Zeitlinger, Lisse, pp. 145-152.
- Bensoussan A., J.L. Lions and Papanicolaou G. (1978) *Asymptotic analysis for periodic structures*, Amsterdam: North-Holland.
- Carde C., R. François, and J. M. Torrenti (1996). Leaching of both calcium hydroxyde and C-S-H from cement paste: modeling the mechanical behaviour. *Cement and Concrete Res.* **28**(6), pp. 1257-1268.
- Gérard B. (1996). Contribution des couplages mécaniques-chimie-transfert dans la tenue à long terme des ouvrages de stockage de déchets radioactifs. Ph. D. thesis, ENS Cachan.
- Humbert P. (1989). CESAR-LCPC, un code général de calcul par éléments finis. *Bull. Liais. Labo. des Ponts et Chaussées* **119**, 112–116.
- Mainguy M., C. Tognazzi, J.M. Torrenti, and F. Adenot (2000). Modelling of leaching in pure cement paste and mortar. *Cement and Concrete Research* **30**, 83–90.
- Nedjar, B. (2002) An enthalpy-based finite element method for nonlinear heat problems involving phase change, *Computers & Structures* **80**, 9-21.
- Nedjar, B., V.H. Nguyen and J.M. Torrenti (2003) A chemo-mechanical modelling framework of concrete: Coupling between calcium leaching and continuum damage mechanics, In N. Bicanic et al. (eds.), *Proc. Euro-C 2003, Computational Modelling of Concrete and Structures*, pp. 559-568. Balkema, Rotterdam, The Netherlands.
- Sanchez-Palencia, E. (1980) *Non-homogeneous media and vibration theory*, Lecture Note in Physics 127, Berlin: Springer-Verlag.
- Torrenti J.M., O. Didry, J P. Ollivier, and F. Plas (1999). La dégradation des bétons – couplage fissuration-dégradation chimique, Hermès.
- Torrenti J.M., M. Mainguy, F. Adenot, and C. Tognazzi (1998). Modelling of leaching in concrete. In R. de Borst, N. Bicanic et al. (eds.), *Proc. Euro-C 98, Computational Modelling of Concrete Struct.*, pp. 531–538. Balkema, Rotterdam, The Netherlands.
- Ulm F.J., E. Lemarchand, and F.H. Heukamp (2002). Elements of chemomechanics of leaching of cement-based materials at different scales. *Engng. Frac. Mechanics in press*.
- Ulm F.J., J.M. Torrenti, and F. Adenot (1999). Chemoporoplasticity of calcium leaching in concrete. *Journal of Engineering Mechanics (ASCE)* **125**(10), 1200–1211.